Conference Proceedings

Solar World Congress 2015
Daegu, Korea, 08 – 12 November 2015

Comparison between the Experimental and the Extrapolated Stagnation Temperature – A Data Base Evaluation

Julian David Hertel[1], Víctor Martínez-Moll[1], Ramon Pujol-Nadal[1], Xabier Olano Martiarena[2], Alberto García De Jalón[2], Fabienne Sallaberry[2]

[1]Departament de Física, Universitat de les Illes Balears, Ctra de Valldemossa km 7,5, 07122 Palma de Mallorca, Illes Balears, Spain

[2]CENER (National Renewable Energy Center), Solar Thermal Energy Department, C/ Ciudad de la Innovación 7, 31621 Sarriguren, Navarra, Spain

Tel: +34 971259542, Fax: +34 971173426, julian.hertel@uib.es

Abstract

Well-designed liquid heating Flat Plate Collectors (FPC) or Evacuated Tube Collectors (ETC) could be used to provide heat at medium temperature levels for industrial processes. According to the most recent ISO 9806:2013 testing standard, the efficiency curve of a collector is constructed by a weighted least square fitting (WLS) based on at least four observations at temperatures spaced over the operating temperature range of the collector. This could lead to poor efficiency predictions at higher operating temperatures, since in this region the fit is not backed up by experimental data. To improve results in the extrapolated area without any additional experimental effort an extended observation fitting could be used, including the collector's stagnation temperature as an additional node point.

Two databases have been evaluated. One database was provided by the National Renewable Energy Centre in Spain (CENER), the other one by the Institute for Solar Technologies (SPF) in Switzerland. It has been shown that in the case of conventional FPCs the extrapolated stagnation temperature from the conventional 8-point fitting constantly underestimates the measured stagnation temperature. In the case of ETCs, on the other hand, the conventional approach leads to an overestimation.

Keywords: *IAM, Factorization, Collector testing, Medium temperature collectors, Industrial heat*

1. Introduction

The industry sector with its high and constant energy demand shows a remarkable potential for the integration of solar thermal technologies. However, beside this potential, current industrial processes still rely on conventional energy supply. Even though, in most cases, the exploitation of available solar resources is economically feasible and profitable, the unreliability and unpredictability often associated with solar energy restrict the companies from investing in new supplementary facilities. Nevertheless solar heat for industrial processes is on the rise.

The IEA task 49 created a database of operating plants to track the development of this sector. Apart from the numerous undocumented examples, the database currently counts 155 commissioned solar plants with a total capacity around 100 MW and 143,000 m^2 in size (Task 49, 2015). Projects are reported all over the world, increasing every year. Most of these plants rely on conventional flat plate and evacuated tube technology at moderate temperature levels below 100 ºC.

The temperature requirements of most industrial processes range from 60 to 260 ºC (Kalogirou, 2003). A significant share of such medium temperature processes could in theory be provided by well-insulated flat plate collectors (FPC) and evacuated vacuum tube collectors (ETC), that so far have mostly been deployed for domestic applications. Both collector types withstand operating conditions far beyond atmospheric pressure and are therefore capable of providing process heat at temperature levels above 100 ºC. Stagnation

temperatures of conventional FPCs are around 200 ºC; those of ETC can reach even higher values, depending on the design (SPF, 2015).

According to the ISO 9806:2013 standard, the efficiency curve of the collector is based on observations at temperature levels evenly spaced over the operating temperature range of the collector. This operating range is usually below 100 ºC when operating at non-pressurized conditions. As a consequence, this approach could lead to an extrapolated area of the efficiency curve which shows larger uncertainties (see Fig. 1).

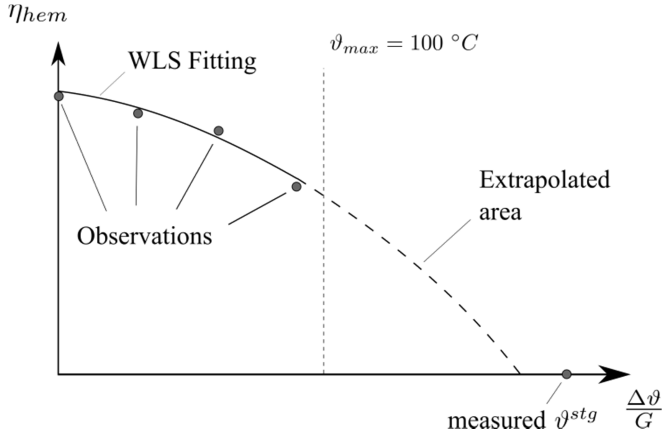

Fig. 1: Standard test procedure: At least four different experimental observations are needed to obtain the collector parameters from a WLS fitting.

One possibility to improve the accuracy of the high temperature part of a collector's efficiency curve could be to include the stagnation temperature in the fitting. The determination of the stagnation temperature forms also part of the standardized test procedure. This way, the methodology could allow improving results without any additional experimental effort.

This is meant to be a preliminary study. The feasibility of this study has been assessed by comparing both the extrapolated (not taking into account the stagnation temperature) and interpolated (taking into account the stagnation temperature) efficiency curve. To do so, three different datasets of FPCs and ETCs from two different databases have been considered. One FPC database was provided by CENER (CENER, 2015), the other two datasets consisting of FPC and ETC collectors were taken from the publicly available database of the Institute for Solar Technology (SPF, 2015). In a second step, the extrapolated stagnation temperature has been compared with the experimentally measured stagnation temperature.

Interestingly results showed a technology specific trend. It could be observed that the difference between measured and extrapolated stagnation temperature is constantly positive in the case of FPC collectors and constantly negative in the case of ETC collectors. To judge the accuracy of the new interpolated efficiency curve, experimental data is essential, which at this point is not available.

2. Collector model and standard testing regulations

In this section the collector model, the collector efficiency curve and the stagnation temperature assessment procedure are described the same way as they are defined in the standard.

2.1. Collector Efficiency Curve

The ISO 9806:2013 (ISO, 2013) is the international and currently most recent version of solar collector testing standard that includes most parts of the former European (CEN, 2006) and American standard (ANSI/ASHRAE, 2003). According to the ISO 9806:2013 standard, the performance of a collector can be characterized by its efficiency curve derived either under steady state or quasi-dynamic conditions. In the case of non-concentrating collectors that are not sensible to direct solar irradiation only, it is common practice to apply the steady state approach according to Eq. (1) (ISO, 2013).

$$\eta_{hem} = \eta_{0,hem} - a_1 \frac{\Delta\vartheta}{G} - a_2 G \left(\frac{\Delta\vartheta}{G}\right)^2 \quad (1)$$

with $\Delta\vartheta$ the temperature difference $\vartheta_m - \vartheta_a$. Where ϑ_m is the mean temperature of the heat transfer fluid (HTF) and ϑ_a is the ambient temperature. $\Delta\vartheta/G$ and $\Delta\vartheta^2/G$ are the explanatory variables of the collector efficiency curve, with G as the hemispherical solar irradiance.

Now, to characterize the collector's efficiency behavior, η_{hem} needs to be measured at least four times, each time at a different quantity $\Delta\vartheta/G$. An analytical expression according to equation (1) is then obtained by determining the characteristic constants $\eta_{0,hem}$, a_1 and a_2 applying a weighted least square fitting (WLS).

The ratio $\Delta\vartheta/G$ for different observations during the test is usually kept small to guarantee accurate fit in temperature regions the collector will most likely be operating on. This means, however, that for collectors that would possibly operate on higher $\Delta\vartheta/G$ -ratios, the fitted efficiency curve is not backed up by experimental data. Output predictions at this region could therefore be inaccurate.

Eq. (1) can be restructured to an energy output per collector area equation, when multiplying by the reference irradiance G. This form of the equation is discussed in Fig. 4.

$$\frac{\dot{Q}}{A} = \eta_{0,hem} G - a_1 \Delta\vartheta - a_2 \Delta\vartheta^2 \quad (2)$$

2.2. Stagnation Temperature Measurement Procedure

To overcome the problem of a lack of observations for higher temperatures without additional experimental effort, it may be useful to include the stagnation temperature as an additional node point in the fitting. For safety reasons (danger of collector over-heating), the stagnation temperature (ϑ_{stg}) is always provided alongside other collector data.

According to the ISO 9806:2013 standard, the stagnation temperature is defined as the highest temperature ϑ_{sm} that can be found on the absorber surface, while the collector is exposed to the available solar irradiance G_m and ambient temperature ϑ_{am} (outdoors, or in a solar irradiance simulator) under steady-state conditions without heat extraction from the collector (stagnation condition). To achieve these conditions with liquid heating collectors, it is recommended to drain the collector completely from all remaining heat transfer fluid and to seal all fluid pipes except for one to prevent cooling by natural circulation.

There is a standardized form of the stagnation temperature which is obtained by assuming a constant proportion of $\vartheta_s - \vartheta_a/G$. With the standard reference values $\vartheta_{as} = 30\ ºC$ and $G_s = 1000\ W/m^2$ according to Eq. (3), the standard stagnation temperature results in:

$$\vartheta_{stg} = \vartheta_{as} + \frac{G_s}{G_m}(\vartheta_{sm} - \vartheta_{am}) \quad (3)$$

Following these guidelines, the test demands that for FPCs the temperature sensor shall be positioned at two-thirds of the absorber height and half the absorber width (see Fig. 2), as it is supposed to be the point on the absorber surface where the temperature is highest during stagnation (ISO, 2013).

For ETCs the specifications are less strict. The ISO 9806:2013 states that in this case the temperature sensor should be placed at a suitable location in the collector, i.e. where the highest temperature relevant to the heat transfer fluid is to be found. Since, in the case of ETCs the absorber surface is not easily accessed, it is common practice to measure the stagnation temperature for a single tube at the tip of the pipe or copper tube respectively (see Fig. 2).

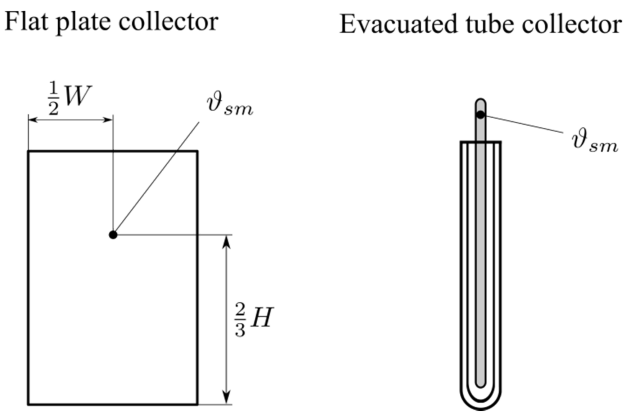

Fig. 2: Stagnation temperature measurement points according to the ISO 9806:2013, with W and H the width and the height of the flat plate collector respectively.

2.3. Collector model

When talking about using the stagnation point as an additional observation for the WLS fitting, attention should be paid to the mathematical model the efficiency curve is based on. Basically, the collector efficiency curve describes the heat transfer mechanisms within the system resulting in a fraction of useful heat and a fraction of heat losses. Fig. 3 illustrates this energy flow with the help of a resistance scheme as an analogy of an electric circuit. The scheme represents a collector with tube absorber. Q^{opt} is the energy flux in form of irradiation as it passes through the optical device. Q^{th} summarizes the heat losses consisting of radiation and convectional losses. The heat removal factor F' plays an important role in this study, as it represents the capacity of the system to transport heat from the absorber surface to the HTF. It takes into account the flow regime and absorber geometries. During stagnation the temperature ϑ_m of the absorber and ϑ_s on the absorber surface are supposed to be equal, since no heat is removed and enough time was given to reach an equilibrium of temperatures.

It is not trivial to say to what extent it is valid to assume that the stagnation point should form part of the efficiency curve. Even though heat transfer mechanisms for a drained collector differ significantly from those of an operating one with constant flow rate, the stagnation temperature measured in both cases should be the same. As Fig. 3 suggests, it is assumed that in case of stagnation there is no heat transport from the collector surface to the HTF. The absorbed energy Q^{opt} is lost completely in form of radiation and convection to the environment. It may therefore be assumed that the stagnation point should form a valid observation for the efficiency curve fitting.

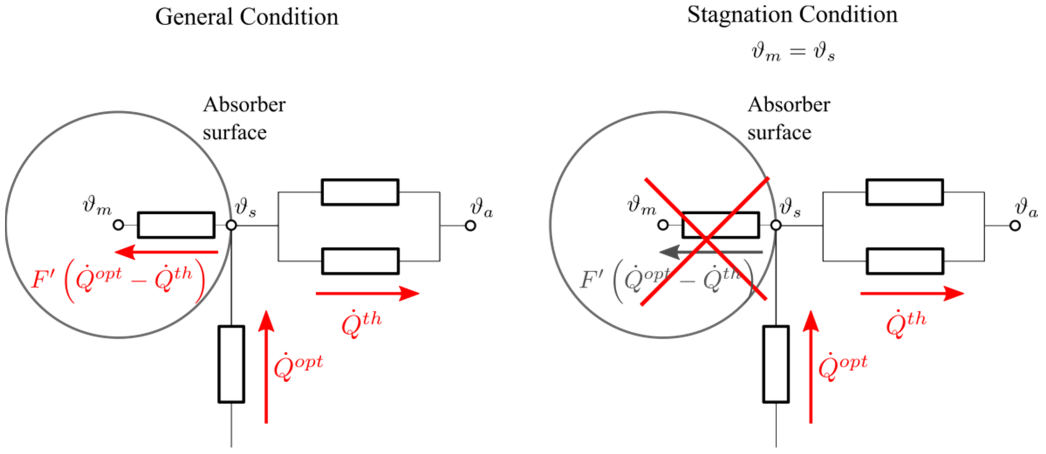

Fig. 3: General heat transfer mechanisms of a solar thermal collector during general operation and stagnation.

3. Method

Three datasets from two different databases have been evaluated. One database was provided by CENER. The database comprises 81 FPCs of different designs. Two more datasets were taken from the database of the Institute of Solar Technology in Switzerland (SPF) consisting of 24 FPCs and 23 ETCs respectively.

As for data provided by CENER, every collector was certified according to the standard regulations with eight data points at four different inlet temperatures. Apart from fitting the collector efficiency curve only to test results for the eight operational modes ($\Delta\vartheta/G$), the stagnation temperature with its typical efficiency of zero has been included as an additional observation as well.

The ISO 9806:2013 standard suggests a WLS fitting. Since uncertainty values of the temperature sensors were not available, it was applied a common multiple linear regression (MLR) fitting instead of the suggested WLS method. This will not make any difference to the outcome of the study.

The collector efficiency equation of Eq. (2) can be converted into a multidimensional linear equation, such that it takes the form of the following general expression:

$$y_i = \beta_0 + \beta_1 x_{i,2} + \beta_2 x_{i,2} + \ldots + \beta_{p-1} x_{i,p-1} + \varepsilon_i \tag{4}$$

with y and x as the experimental parameters or observations, β as the regression coefficients and ε as the error. According to the MLR approach there exists a set of regression coefficients which minimizes the overall error $\sum_{i=1}^{n} \varepsilon_i$. This optimal coefficient vector is given by:

$$\widehat{\boldsymbol{b}} = (\boldsymbol{X}^T \boldsymbol{X})^{-1} \boldsymbol{X}^T \boldsymbol{Y} \tag{5}$$

where $\boldsymbol{b}$ is the vector of the regression coefficients.

$$\boldsymbol{b} = \begin{bmatrix} \beta_0 \\ \vdots \\ \beta_p \end{bmatrix} = \begin{bmatrix} \eta_0 \\ a_1 \\ a_2 \end{bmatrix} \tag{6}$$

applying this Eq. (1), the design parameters which need to be determined are the optical efficiency η_0 and the thermal coefficients $a$and a. **X** is a n × p -matrix that contains the n observations for each parameter p.

$$\boldsymbol{X} = \begin{bmatrix} 1 & x_{1,1} & \cdots & x_{1,p-1} \\ \vdots & \vdots & \ddots & \vdots \\ 1 & x_{i,1} & \ldots & x_{i,p-1} \\ \vdots & \vdots & \ddots & \vdots \\ 1 & x_{n,1} & \ldots & x_{n,p-1} \end{bmatrix} = \begin{bmatrix} 1 & \frac{\Delta\vartheta_1}{G} & \frac{{\Delta\vartheta_1}^2}{G} \\ \vdots & \vdots & \vdots \\ 1 & \frac{\Delta\vartheta_i}{G} & \frac{{\Delta\vartheta_i}^2}{G} \\ \vdots & \vdots & \vdots \\ 1 & \frac{\Delta\vartheta_n}{G} & \frac{{\Delta\vartheta_n}^2}{G} \end{bmatrix} \tag{7}$$

In the case of Eq. (1) these parameters are the constant 1 and the experimental results for $\Delta\vartheta_1/G$ and ${\Delta\vartheta_1}^2/G$. $\boldsymbol{Y}$ is also a vector of observations containing the experimental results of the collector efficiency η.

$$\boldsymbol{Y} = \begin{bmatrix} y_1 \\ \vdots \\ y_i \\ \vdots \\ y_n \end{bmatrix} = \begin{bmatrix} \eta_1 \\ \vdots \\ \eta_i \\ \vdots \\ \eta_n \end{bmatrix} \tag{8}$$

Apart from the regular fit, the 95%-confidence region has been calculated in order to analyze the accuracy of the fit and see how far the 8-point and 9-point fit are statistically apart. The 95%-confidence margin of a regression parameter is defined as

$$\beta_i^{conf} = \beta_i \pm t^*_{n-p,1-\alpha/2} \sqrt{\widehat{\boldsymbol{V}}(\boldsymbol{b})_{ii}} \tag{9}$$

with α as the confidence parameter; $\alpha = 0.05$. $t^*_{n-p,1-\alpha/2}$ is the t-value of the Student's *t*-distribution and $\widehat{\boldsymbol{V}}(\boldsymbol{b})_{ii}$ are the diagonal elements of the estimated variance-covariance matrix. The variance-covariance matrix is defined as

$$\widehat{\boldsymbol{V}}(\boldsymbol{b}) = MSE(\boldsymbol{X}^T \boldsymbol{X})^{-1} \tag{10}$$

where MSE is the mean square error of the error ε_i:

$$MSE = \sum_{i=1}^{n} (\boldsymbol{Y} - \boldsymbol{Xb})^2 \tag{11}$$

For the discussion in section 4 both efficiency curves, the 8-point fit and 9-point fit, have been plotted together with the 95%-confidence interval of the regression coefficient vector $\boldsymbol{b}$.

The SPF database already provides all efficiency curve parameters as well as the measured stagnation temperature. It was therefore not necessary to apply a MLR fitting and it was not possible to analyze the 95% confidence interval of the curve. Instead, only the difference between the measured stagnation temperature and the stagnation temperature suggested by the efficiency curve were compared with each other. This comparison also forms part of the discussion of the results obtained by the CENER data evaluation.

4. Results

4.1. CENER Database

The database comprises 81 FPCs of different design. The collectors were tested according to the ISO 9806:2013 standard regulations. Data therefore includes eight observations at four different temperature levels as well as the stagnation temperature. Based on this information one representative example has been chosen to compare two different efficiency curve fits with each other. One efficiency curve is based on the eight regular observations, while the other one also includes the stagnation point as an additional node point.

Fig. 4 shows the results for the 8-point (not including the stagnation point) and 9-point fit (including the stagnation point) of the selected collector. Beside the efficiency curves, the 95%-confidence region is indicated by dashed lines. The confidence range was determined according to Eq. (9). Interestingly, the extrapolated stagnation temperature ϑ_{fit} differs significantly from the measured stagnation temperature ϑ_{stg}. In this specific example the difference $\vartheta_{stg} - \vartheta_{fit}$ is 48.5 ºC.

The 95%-confidence margin also indicates that the difference between both values is too large as to be explained by statistical accuracy of the fit. ϑ_{stg} lies far outside the 95%-confidence region. In some parts an overlap can be observed between the 95%-confidence uncertainty margins of both curves.

At this stage of research it is not possible to say which of the two curves represents the real collector behavior better. What should be noted regarding the 9-point fit is a less-realistic shape of the curve. Its curvature is opposed to the one obtained by the regular collector efficiency behavior.

The most probable solution to the real collector efficiency curve is somewhere in-between the two presented curves. In order to validate the suggested 9-point fit it is essential to obtain observations for the medium and high temperature range.

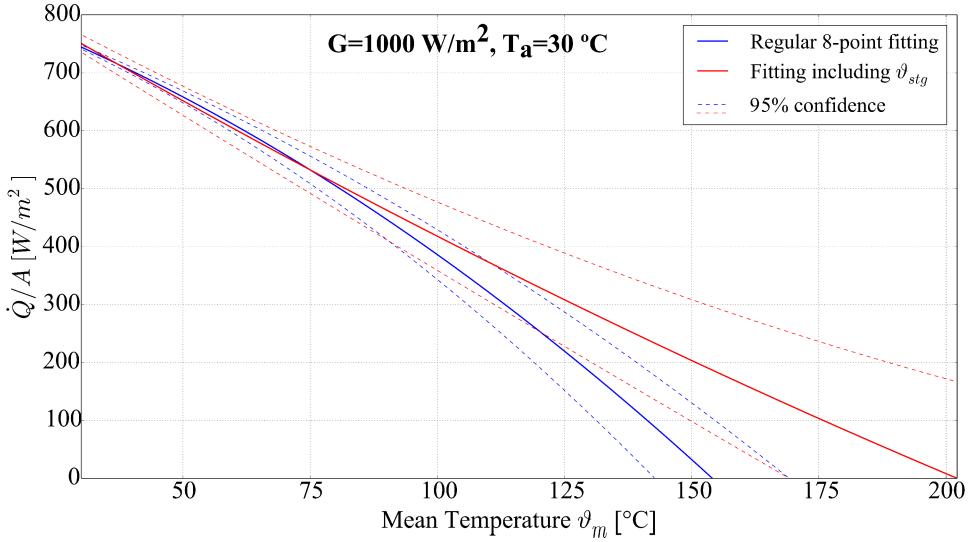

Fig. 4: Comparison of a regular 8-point fit with a 9-point fit that includes the stagnation temperature. A multiple linear regression fit (MLR) was applied to a flat plate collector with solar glass cover, aluminum plate absorber, and isolated with rock wool.

Fig 5 shows the distribution of temperature differences $\vartheta_{stg} - \vartheta_{fit}$ as they were found for all collectors of the database. Extrapolated stagnation temperature ϑ_{fit} from the 8-point fit is constantly underestimating the measured one. While the average gap is 39.47 ºC in one case it even reaches 83 ºC.

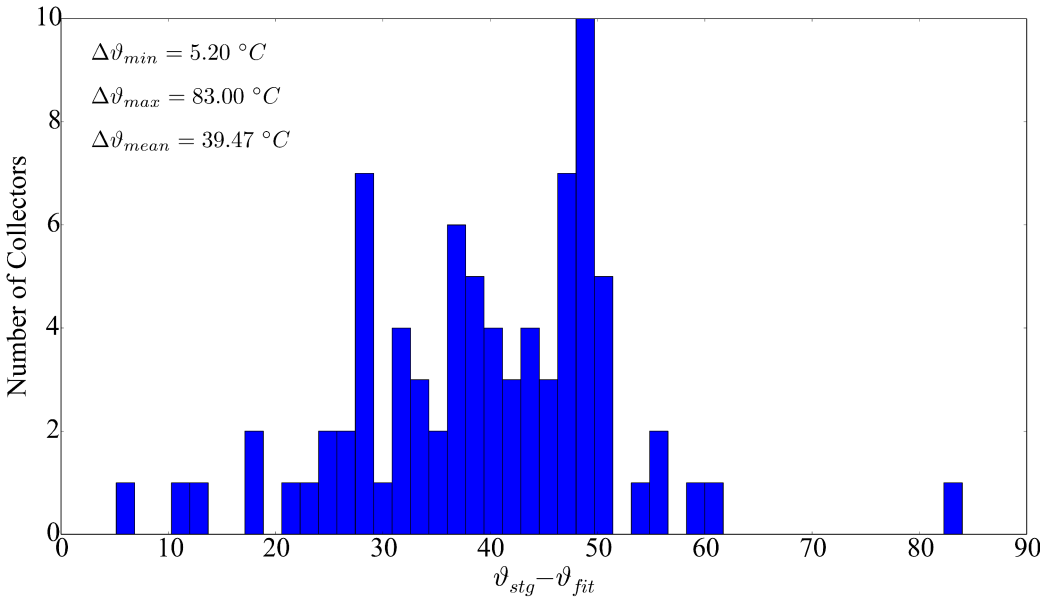

Fig. 5: Distribution of the difference between the actually measured stagnation temperature ϑ_{stg} and the estimated stagnation temperature ϑ_{fit}. The distribution represents results for 81 flat plate collectors certified by CENER.

4.2. SPF Database

SPF provides an extensive database of test results of FPCs and ETCs that is publicly available. Two datasets based on this database have been evaluated in this study. The datasets consist of 24 FPCs and 23 ETCs respectively.

As can be seen in Fig 6, results for FPCs show almost constantly positive temperature differences $\vartheta_{stg} - \vartheta_{fit}$ same as was reported for the CENER database. The maximum temperature difference found was 26.30 ºC. However, in three cases the measured stagnation temperature seems to be well represented by the extrapolated one.

As an interesting fact, it could be shown that in the case of ETCs the gap $\vartheta_{stg} - \vartheta_{fit}$ is negative in most of the cases. The extrapolated value is consequently overestimating the measured stagnation temperature. Especially in two cases a very large difference of -159.74 ºC could be found. It should be noted that one of the reasons for this negative temperature difference could be the way in which the stagnation temperature is measured for ETCs. Since it is often complicated to attach temperature sensors to the absorber surface inside the evacuated tube, the sensor is placed at the heat of the tube. Taking into consideration the temperature gradient along the tube as a result of heat transport mechanisms, a lower temperature can be expected at the tip of the tube than further down at towards the bottom.

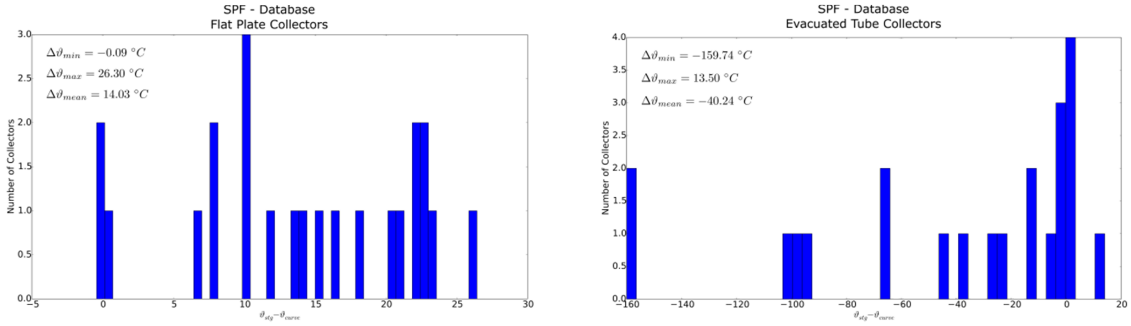

Fig. 6: Absolute distribution of the difference between the actually measured stagnation temperature ϑ_{stg} and the estimated stagnation temperature ϑ_{fit}. The distribution represents results for 24 FPCs and 23 ETCs from the SPF database.

5. Conclusion and Outlook

The conventional data fitting approach according to the ISO 9806:2013 standard constantly underestimates the actual stagnation temperature in the case of FPCs and overestimates it in the case of ETCs. The reason for these differences is most likely due to the way the stagnation temperature is measured. Stagnation temperature assessment methods differ for every type of technology. In addition, the accuracy of the measured stagnation temperature might depend on a couple of other effects such as the temperature dependency of optical properties and non-linear effects of convectional heat transfer.

An exemplary sample from the CENER database showed that since ϑ_{stg} was found outside the fit's 95-confidence interval; in this case statistical errors of the prediction could be excluded. In some parts an overlap was observed between the 95%-confidence uncertainty margins of both curves.

Whether a 9-point fit could yield more accurate results within the high temperature range of the efficiency curve is not straight forward to say. It will be necessary to validate this approach with experimental data at higher operating temperatures. This will be done in a further study. An evaluation of the results will show, whether the integration of ϑ_{stg} into WLS fitting is physically reasonable.

6. References

ANSI/ASHRAE, 2003. ASHRAE Standard 93 Methods of Testing to Determine Thermal Performance of Solar Collectors.

CEN, 2006. EN 12975-2. Thermal solar systems and components – Solar collectors – Part 2: Test methods. European Committee for Standardisation.

CENER, 2015. National Renewable Energy Centre, Spain (CENER) [WWW Document]. URL http://www.cener.com/en/ (accessed 9.27.15).

ISO, 2013. Solar energy - solar thermal collectors - test methods, ISO (Ed.) ISO 9806:2013(E).

Kalogirou, S., 2003. The potential of solar industrial process heat applications. Appl. Energy 76, 337–361. doi:10.1016/S0306-2619(02)00176-9

SPF, 2015. Institute for Solar Technology [WWW Document]. URL http://www.spf.ch/Home.44.0.html?&L=6 (accessed 9.27.15).

Task 49, 2015. SHIP database [WWW Document]. URL http://ship-plants.info/ (accessed 9.27.15).